CHARGE BREEDING EXPERIENCES WITH ECR AND EBIS FOR CARIBU

Richard Vondrasek[#], A. Barcikowski, C.A. Dickerson, P.N. Ostroumov,
R. Pardo, A. Perry, G. Savard, R. Scott, S.I. Sharamentov
Physics Division, Argonne National Laboratory, Lemont, IL 60439, USA

Abstract

The efficient and rapid production of a high-quality, pure beam of highly charged ions is at the heart of any radioactive ion beam facility. An ECR charge breeder, as part of the Californium Rare Ion Breeder Upgrade (CARIBU) program at Argonne National Laboratory, was developed to fulfil this role. The charge breeding efficiency and high charge state production of the source are at the forefront of ECR charge breeders, but its overall performance as part of the accelerator system is limited by a pervasive stable ion background and relatively long breeding times. Steps have been taken to reduce the level of background contamination but have met with limited success. As such, an EBIS charge breeder has been developed and is now running in an off-line configuration. It has already demonstrated good breeding efficiencies, shorter residence times, and reduced background, and it is scheduled to replace the ECR charge breeder in late 2015. The resultant change in duty cycle and time structure necessitates changes to the overall facility operation. The experiences with these breeders – their strengths and their weaknesses - will be discussed.

CARIBU FACILITY

The CAlifornium Rare Isotope Breeder Upgrade (CARIBU)[1] provides radioactive beams to the Argonne Tandem Linac Accelerator System (ATLAS). The fission fragments are produced not by an ISOL facility but instead by a 1.3 Ci ^{252}Cf fission source. The Cf source is located inside a large-volume RF/DC helium gas catcher [2] which thermalizes the fission products and extracts them rapidly to form a low-energy beam of 1+ or 2+ ions from which the isotopes of interest are selected via a high-resolution magnetic separator. The beam is transported to either a low-energy area which includes a Penning trap and tape station or to an ECR source where the beam is charge bred for subsequent acceleration in the ATLAS linac.

The ECR breeder has been delivering charge bred radioactive species to the ATLAS experimental program for several years and in the last year has provided more than 81 days of beam. While its charge breeding efficiency and high charge state production have been at the forefront of ECR charge breeding, its overall performance as a part of the accelerator system has been hindered by the pervasive background present in ECR ion sources.

As such, an EBIS charge breeder is replacing the ECR in late 2015. The EBIS has a lower level of beam contam-

_____
#vondrasek@anl.gov

ination than an ECR and exhibits improved charge breeding efficiency and faster breeding times [3, 4].

ECR CHARGE BREEDER

The ANL ECR breeder [5] is a room temperature source, and the plasma is excited with two RF frequencies – a 10.44 GHz klystron and an 11-13 GHz traveling wave tube amplifier (TWTA). It has an open hexapole structure providing good pumping to the plasma chamber region resulting in a base plasma chamber pressure of 2×10^{-8} mbar. The open structure also allows the RF and support gas to be introduced radially into the plasma chamber. This scheme eliminates the need for cut-outs in the field shaping iron to accept the RF waveguides and results in a highly symmetric axial magnetic field where the ions enter the plasma. This differs from other ECR breeders presently in existence which are closed hexapole devices with axial RF injection. The 1+ ions are introduced into the plasma through a grounded high-purity aluminum tube mounted on a linear motion stage. The stage has a 30 mm range of travel, and thus the deceleration point of the 1+ ions can be adjusted on-line without disturbing the source conditions. The source is designed to operate at a 50 kV potential although it typically operates at 36 kV. The source has produced beams primarily in the mid-mass regime but has also exhibited good performance for low mass beams such as sodium and potassium (see Table 1).

Table 1: Summary of Charge Breeding Performance for Both Stable Ions and CARIBU Provided Radioactive Ions

Ion	Half-life (s)	Efficiency (%)	A/Q
^{23}Na^{7+}		10.1	3.29
^{39}K^{10+}		17.9	3.90
^{84}Kr^{17+}		15.6	4.94
^{85}Rb^{19+}		13.7	4.47
^{110}Ru^{22+}	11.6	11.8	5.00
^{135}Te^{26+}	19.0	5.0	5.19
^{129}Xe^{25+}		13.4	5.16
^{132}Xe^{27+}		14.1	4.89
^{133}Cs^{26+}		14.7	5.11
^{133}Cs^{27+}		13.5	4.93
^{141}Cs^{27+}	24.8	12.3	5.22
^{142}Cs^{27+}	1.69	7.3	5.26
^{143}Cs^{27+}	1.79	11.7	5.30
^{143}Ba^{27+}	14.3	14.7	5.30
^{144}Ba^{28+}	11.5	14.3	5.14
^{146}Ba^{28+}	2.22	13.3	5.21

Charge Breeder Enhancements

The performance of the ANL ECR charge breeder can be attributed to several aspects: the open hexapole which

allows better pumping to the plasma chamber region, the symmetric magnetic field at the point of 1+ ion injection, and multiple frequency heating.

The beneficial effect of a lower operating base pressure was first observed with rubidium through improved breeding efficiencies and peak charge state as a function of source pressure. Table 2 shows the breeding efficiencies for two periods – September 2008 when the operating pressure was 2.0×10^{-7} mbar and June 2009 when the pressure was 1.0×10^{-7} mbar. Source conditions, other than the pressure, were the same for both data sets.

In addition to better pumping, the open hexapole structure also allowed the RF waveguides to be inserted in between the hexapole bars. This resulted in a symmetrical iron plug on the injection side of the source which maintained the magnetic field symmetry where the 1+ ions enter the chamber.

Table 2: Summary of Charge Breeding Performance for Both Stable Ions and CARIBU Provided Radioactive Ions

Ion	Efficiency (2.0e-7 mbar)	Efficiency (1.0e-7 mbar)
$^{85}Rb^{11+}$	0.8	-
$^{85}Rb^{13+}$	1.8	-
$^{85}Rb^{15+}$	3.8	3.8
$^{85}Rb^{17+}$	0.8	5.2
$^{85}Rb^{19+}$	-	3.2
$^{85}Rb^{20+}$	-	2.9

1+ Ion Injection

Computer Simulation Technology Electromagnetic Studio was used to simulate 3D ion injection into the ECRCB using the source running conditions for the magnetic fields, electric potentials, and a ΔV potential of -10 V. The simulations did not take into account plasma collisional effects. Ions of Na^+, K^+, and Cs^+ were flown into the ECRCB plasma chamber and their depth of penetration was tracked. Cases were simulated for the symmetric iron configuration as well as a configuration in which the RF was launched on axis thus necessitating cut-outs in the injection iron and resulting in an asymmetric magnetic field. The simulation results are shown in Fig. 1. In the plot, the 0 cm position is defined as the end of the grounded tube where the 1+ ions enter the plasma chamber. The peak axial magnetic field on the injection side (B_{max}) is located at 8 cm. The chamber mid-point is at 23 cm (B_{min}), and the extractor is at 38 cm (B_{ext}). In all of the symmetrical iron cases, 100% of the injected 1+ ions penetrated past the B_{max} location, and 40-55% of the total injected ions penetrated as far as the extraction electrode. In the asymmetrical cases, 60-90% of the
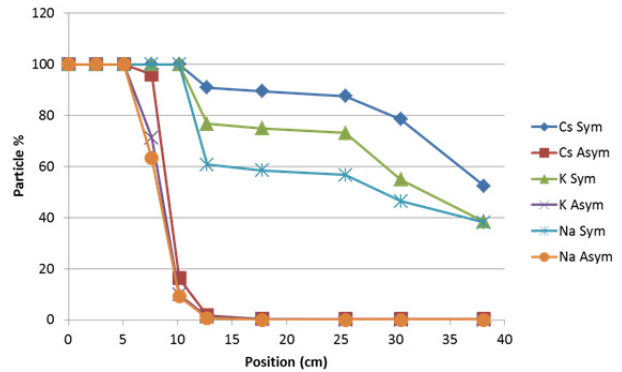

Figure 1: Simulated penetration of injected 1+ ions into ECR plasma chamber for symmetric (Sym) and asymmetric (Asym) iron cases.

injected 1+ ions penetrated past the B_{max} point, but only 1-2% passed the 13 cm mark and no ions reached the mid-point of the chamber. It is believed that this lack of penetration into the plasma region can hinder the capture of the 1+ ions and thus reduce the breeding efficiency. Recent modifications to the SPIRAL Phoenix charge breeder appear to support this conclusion [6]. The injection iron configuration was modified to eliminate field asymmetries where the 1+ ions enter the plasma chamber. In off-line testing, the source has demonstrated high breeding efficiencies including for the low mass species.

Multiple Frequency Heating

The first test of multiple frequency heating's effect on breeding efficiency was with ^{129}Xe. Three RF schemes were investigated: 1) klystron only, 2) TWTA only, 3) klystron+TWTA. To serve as a direct comparison of the various RF injection schemes, the total RF power launched into the source was kept constant at 245 W, only the power distribution between the klystron and TWTA was varied. With the source running an oxygen plasma and an extraction voltage of 20 kV, a 65 nA beam of $^{129}Xe^+$ was injected into the ECRCB and the breeding efficiency measured as a function of RF power distribution with the results shown in Fig. 2. When going from single to two-frequency heating, the peak of the
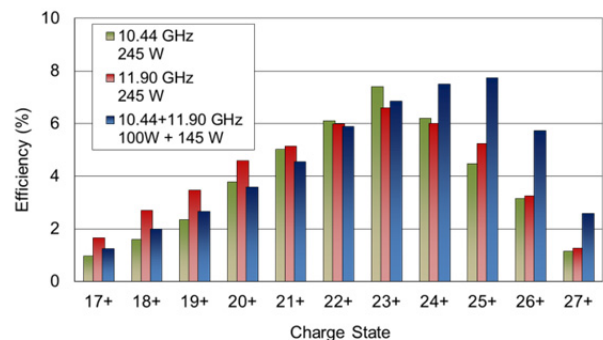

Figure 2: Simulated penetration of injected 1+ ions into ECR plasma chamber for symmetric (Sym) and asymmetric (Asym) iron cases.

charge state distribution shifted from 23+ to 25+ accompanied by a doubling of the breeding efficiency for 26+ and 27+.

Charge Breeding Time

It was observed that changes in the charge breeding efficiency due to RF power levels and operating frequency could be accompanied by dramatic changes in the charge breeding time. Fig 3 shows the observed efficiencies and rise times for ^{132}Xe as a function of the TWTA operating frequency. The ^{132}Xe$^+$ was provided by an RF discharge source with an intensity of 17 enA. The ECRCB was run with an oxygen plasma and single frequency heating employing only the TWTA. When the frequency of the TWTA was shifted from 11.762 GHz to 11.765 GHz (300 W) several effects were observed: 1) the charge state distribution shifted to higher charge states, 2) the breeding efficiencies for the high charge state ions increased, 3) the charge breeding times increased. No other source parameters were changed between these two data sets implying that the frequency shift was the sole cause of the change in the plasma properties, possibly due to a change in the plasma potential as observed in Ref. [7]. Clearly the choice of operating frequency is just as critical with charge breeding as has been demonstrated in normal ECR operation [8]. While the exact mechanism of the operating frequency effect is still being investigated, it does give the source operator another convenient knob with which to optimize the ion source performance.
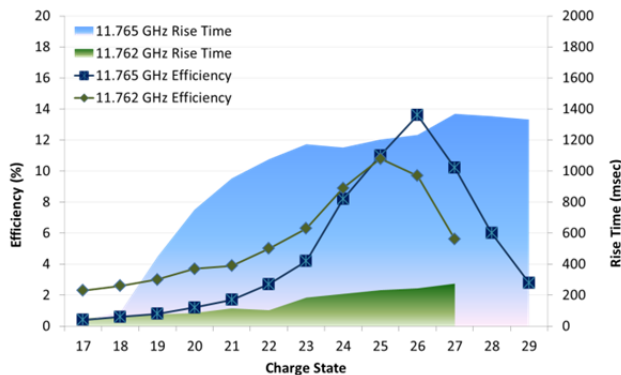

Figure 3: Xe-132 breeding efficiencies and rise times for TWTA operating frequencies of 11.762 GHz (in green) and 11.765 GHz (in blue).

Charge Breeder Background

The ubiquitous background contamination of ECR ion sources is well known [9,10]. Examples of this background are shown in Figs. 4 and 5, silicon barrier detector spectrums of a ^{144}Ba^{28+} and a ^{146}Ba^{28+} beam after acceleration in the ATLAS linac. The ^{144}Ba shows several contaminants (^{36}Ar^{7+}, ^{72}Ge^{14+}, ^{108}Cd^{21+}, ^{180}Hf^{35+}) with the dominant contaminant being ^{36}Ar. In [11], the source of the ^{36}Ar was attributed solely to surface desorption and not o-ring permeation. In that analysis, however, the fact that the permeation rate of Viton increases with temperature was not taken into account and this could also explain the increase in ^{36}Ar rates observed in that
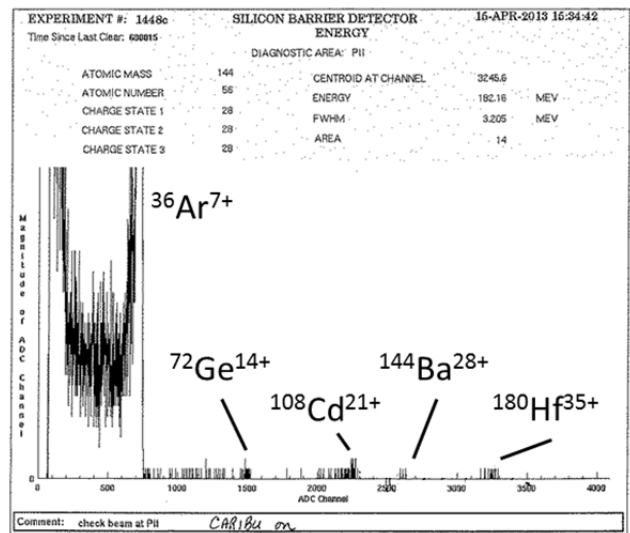

Figure 4: Beam of accelerated Ba-144 and its contaminants observed with a silicon barrier detector.
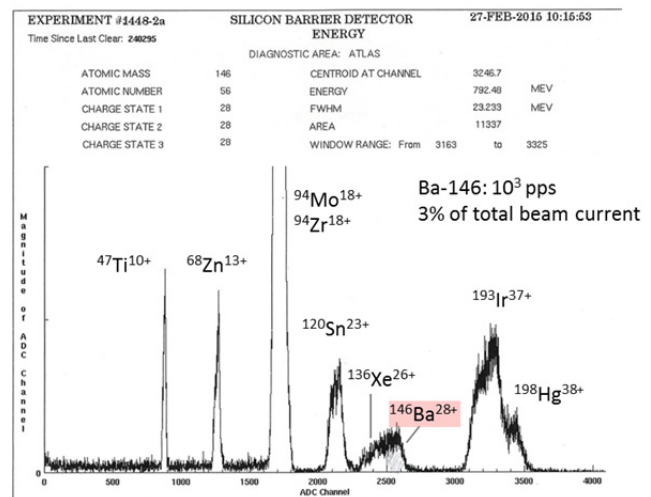

Figure 5: Beam of accelerated Ba-146 and its contaminants observed with a silicon barrier detector.

work. Calculations show that the 17 Viton o-rings on the source produce at room temperature an equivalent leak rate of 10^{-5} torr-l/s limiting the ultimate base pressure of the ion source to 2×10^{-8} mbar. The other species in the spectrum are due to either contamination of the plasma chamber surfaces or the bulk aluminum. The ^{144}Ba peak, while still visible at channel 2600 in the spectrum, represents <0.5% of the overall detector rate.

The impact of surface and bulk material contamination is more clearly seen in the ^{146}Ba spectrum where the stable beam components account for 97% of the total rate into the detector. Titanium and zinc are components of 6061 aluminum, the material used for the plasma chamber body. The source of the molybdenum, tin, iridium, and mercury is less understood. Only 7 contaminants out of a possible 47 [(m/q)/(Δm/q)>300)] are observed, and due to there being no strong contaminant near mass 146, the ^{146}Ba^{28+} radioactive beam component is still easily identified.

Charge Breeder Cleaning

Cleaning of the chamber surfaces with sand blasting and high pressure rinsing has been successfully demonstrated to reduce the background contamination [9]. However, these procedures would necessitate disassembling the ECR ion source and constructing a clean room to ensure a clean environment for source reassembly, and this was not compatible with the accelerator run schedule. It was decided to utilize CO_2 snow cleaning of the plasma chamber surfaces as well as the injection and extraction hardware. It is a non-destructive, non-abrasive, and residue-free method based upon the expansion of either liquid or gaseous carbon dioxide through an orifice leading to the nucleation of small dry ice particles in a high velocity gas carrier stream. The CO_2 pellets remove micron and submicron particulates by momentum transfer and hydrocarbons via a freeze-fracture mechanism. The high-velocity carrier gas propels the contaminants out of the system thus eliminating the need for high pressure rinsing and allowing the entire process to be done in situ.

In order to shield the 6061 aluminum wall from direct exposure to the plasma and thus address the bulk contaminant issue, the chamber was coated with ultra-high purity aluminum (99.9995%). A tungsten coil which had been saturated with the aluminum was suspended in the middle of the plasma chamber. The source was evacuated to 10^{-7} mbar and the coil heated resulting in an average surface deposition of 1 micron. Although not all surfaces were adequately coated, namely an injection side disk and mating piece both of which are constructed of 6061 aluminum, the majority of the plasma chamber was coated.

Before the CO_2 cleaning, a detailed mass scan of the entire source output was performed with analyzing slits set at +/-0.1 mm recording all peaks with an intensity >1 epA. After the CO_2 cleaning, the scan was repeated with the exact same source conditions. We observed reductions in three major observed contaminants – a factor of 20 reduction for fluorine, a factor of 4 for chlorine, and a factor of 50 for iron.

After the aluminum coating, the mass scan was repeated with the same source settings. The three contaminants were further reduced – a factor of 160 reduction for fluorine, a factor of 17 reduction for chlorine, and iron was no longer detectable.

Figure 6 shows silicon barrier spectra taken before and after the aluminum coating. As a result of the coating, several of the stable contaminants observed in the silicon barrier spectrum have either been eliminated (iron, cadmium, cerium) or have come down significantly (titanium). A significant ^{98}Mo peak remains and two new contaminants have been introduced – ^{181}Ta and ^{186}W – presumably due to the tungsten heating coil used for the evaporation which had a 20 ppm component of tantalum and a 10 ppm component of molybdenum. On the experimenter's detector, the ^{98}Mo was reduced by a factor of 5, the ^{142}Ce was eliminated (the Fe and Cd were not observed), but the Ta and W now dominated the spectrum.
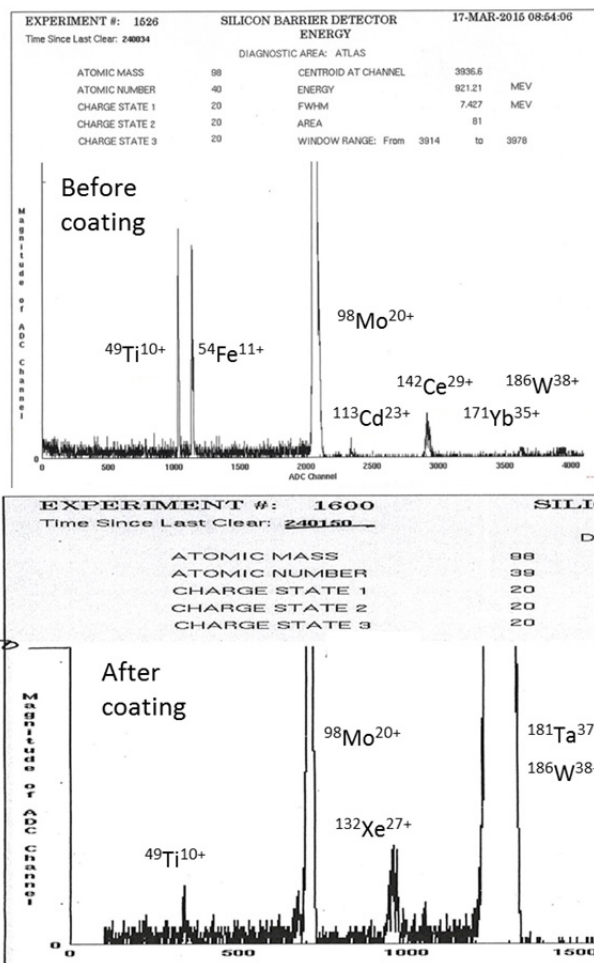

Figure 6: Silicon barrier detector spectra for before and after aluminum coating. The Mo-98 has been reduced by a factor of 5, and the Fe-54, Cd-113, Ce-142 have been eliminated. New contaminants of Ta and W are now present.

While the above techniques have demonstrated significant reductions in the level of background, especially that due to surface contamination, there are several refinements which can be made. The o-rings need to be eliminated from the source design to establish a truly UHV system. This advancement has been incorporated into the construction of the SPIRAL PHOENIX ECR charge breeder. A new technique to evaporate the aluminum needs to be developed. It is possible that a greater reduction in the ^{98}Mo component could have been realized if not for the 10 ppm molybdenum content of the heating coil, as inferred by the significant increase in Ta and W. Several off-line tests with various carbon-based heating elements have been performed with limited success.

EBIS PERFORMANCE

The demonstrated higher efficiencies, shorter breeding times, and greater purity of charge-bred radioactive ion beams achievable with an EBIS have led ANL to develop an EBIS in collaboration with the Brookhaven group [12]. However, the parameters of the electron gun, potential

distribution in the ion trap region, electron collector and injection/extraction beam lines are substantially modified from the Brookhaven design in order to obtain the highest acceptance and breeding efficiency of low intensity rare isotope beams. Special attention was paid to the design of the vacuum system to maintain high purity of the charge-bred radioactive ion beams. Parameters and some design details of the CARIBU EBIS CB are described elsewhere [13].

The first off-line charge breeding results were obtained in May 2014 [14]. With the injection of a Cs^+ beam, a charge breeding efficiency of 10% into 14+ was realized with a modest solenoid field (4 T) and electron beam density (170 A/cm^2). There was still a high level of residual background due to several small vacuum leaks which were eventually identified and fixed.

After performing a multi-day bake-out and utilizing a higher magnetic field (5 T) and electron beam density (385 A/cm^2), the background was substantially lower and we achieved a 20% breeding efficiency into 28+ for 28 ms breeding time, 10^7 ions/pulse without preparation in a cooler/buncher, and a repetition rate of 10 Hz [15] (Fig. 7). For comparison, the best the ECR breeder has achieved is 13% into 27+ with a breeding time on the order of 300 ms.

The EBIS will replace the ECR charge breeder in late 2015. In addition, the beamline on the CARIBU deck will be reconfigured to incorporate an MR-TOF providing greater mass resolution in the 1:40000 range with >50% transmission and a capacity of 10^4 ions/bunch. The system will work at repetition rates between 1-30 Hz. Other than the dipole magnets and a few steerers, all transport elements in the low energy line will be electrostatic. The system is scheduled to be operational in early 2016.
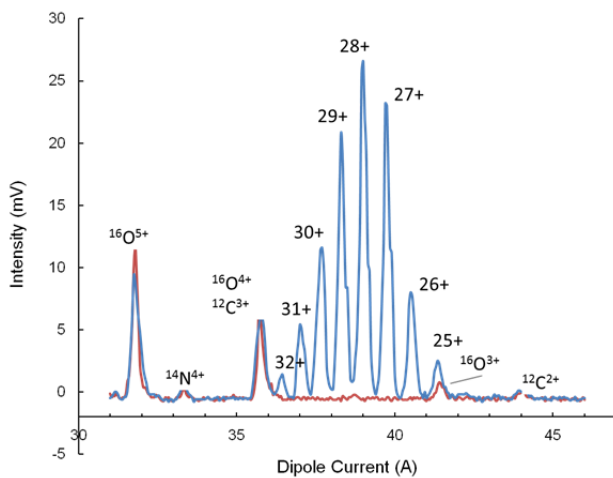

Figure 7: Spectrum of charge bred cesium from the EBIS.

REFERENCES

[1] R. Pardo, G. Savard, S. Baker, C. Davids, E.F. Moore, R. Vondrasek, G. Zinkann, NIM-B 261, Issues 1-2 (2007) 965.

[2] G. Savard, Journal of Physics: Conference Series, 312 (2011), p. 052004.

[3] F. Wenander, Nucl. Instrum. Meth. B266 (2008) p.4346-4353.

[4] P. Delahaye, NIM-B, Volume 317, Part B, 15 December 2013, Pages 389-394.

[5] R.C. Vondrasek, R. Scott, J. Carr and R.C. Pardo, Rev. Sci. Instrum. 79, 02A901 (2008).

[6] L. Maunoury, "Charge breeder for the SPIRAL1 upgrade: preliminary results", ICIS2015, New York, NY, August 23-28, 2015.

[7] O. Tarvainen, P. Suominen, T. Ropponen, and H. Koivisto, Rev. Sci. Instrum. 77, 03A309 (2006).

[8] L. Celona, G. Ciavola, F. Consoli, S. Gammino, F. Maimone, D. Mascali, P. Spädtke, K. Tinschert, R. Lang, J. Mäder, J. Roßbach, S. Barbarin, R.S. Catalano, Rev. Sci. Instrum. 79, 023305 (2008).

[9] N. Imai, S. C. Jeong, M. Oyaizu, S. Arai, Y. Fuchi, Y Hirayama, H. Ishiyama, H. Miyatake, M.H. Tanaka, M. Okada, and Y. X. Watanabe, Rev. Sci. Instrum. 79, 02A906 (2008).

[10] F. Ames, R. Baartman, P. Bricault, K. Jayamanna, T. Lamy, M. McDonald, Rev. Sci. Instrum. 81, 02A903 (2010).

[11] R. Vondrasek, J. Clark, A. Levand, T. Palchan, R. Pardo, G. Savard, R. Scott, Rev. Sci. Instrum.85, 02B903 (2014).

[12] S. Kondrashev, C. Dickerson, A. Levand, P. N. Ostroumov, R. C. Pardo, G. Savard, R. Vondrasek, J. Alessi, E. Beebe, A. Pikin, G. I. Kuznetsov and M. A. Batazova, Rev. Sci. Instrum. 83, 02A902 (2012).

[13] S. Kondrashev, A. Barcikowski, C. Dickerson, R. Fischer, P. N. Ostroumov, R. Vondrasek and A. Pikin, Rev. Sci. Instrum. 85, 02B901 (2014).

[14] S. Kondrashev, A. Barcikowski, C. Dickerson, P.N. Ostroumov, S. Sharamentov, R. Vondrasek and A. Pikin, AIP Conf. Proc. 1640, 54 (2015).

[15] P. Ostroumov, A. Barcikowski , C. Dickerson , A. Perry , A. Pikin , S. I. Sharamentov , R. Vondrasek , G. Zinkann, Rev. Sci. Instrum., Accepted for publication.